JACS
JOURNAL OF THE AMERICAN CHEMICAL SOCIETY

COMMUNICATION

pubs.acs.org/JACS

# Ultrafast Charge Separation and Recombination Dynamics in Lead Sulfide Quantum Dot−Methylene Blue Complexes Probed by Electron and Hole Intraband Transitions

Ye Yang, William Rodríguez-Córdoba, and Tianquan Lian*

Department of Chemistry, Emory University, 1515 Dickey Drive NE, Atlanta, Georgia 30322, United States

Supporting Information

**ABSTRACT:** Lead salt quantum dots (QDs) have emerged as attractive materials for solar energy conversion because of their broad spectral response, long exciton lifetime, and efficient multiexciton generation. However, charge separation dynamics from these QDs remain poorly understood. In this study we investigate charge separation and recombination dynamics in PbS−methylene blue ($MB^+$) complexes by femtosecond transient absorption spectroscopy. We show that while the 1S electrons and holes in excited PbS QDs lead to overlapping transient absorption features in the visible and near-IR regions, their intraband absorptions in the mid-IR can be monitored independently to directly follow the charge separation and recombination processes. The charge separation and recombination rates in PbS-$MB^+$ complexes were found to be $(2.7 \pm 0.2) \times 10^{12}$ and $(1.1 \pm 0.2) \times 10^{11}$ $s^{-1}$, respectively. The ultrafast charge separation rate suggests the possibility of hot electron injection and multiexciton dissociation from these strongly quantum confined QDs, consistent with recent reports of these phenomena at lead salt QD/$TiO_2$ interfaces.

Lead salt (PbS, PbSe, and PbTe) quantum dot (QD)-based solar cells have been intensively investigated in recent years because of the many unique photophysical properties of these materials.[1−4] These properties include tunable and broad spectral responses extending from the visible to near-IR regions,[2,5,6] long exciton lifetimes,[7,8] multiple exciton generation (MEG),[9−12] and hot carrier extraction.[13] MEG and hot carrier extraction provide potential new ways to improve the conversion efficiencies of QD-based solar cells by reducing the loss of high-energy carriers.[14] Parkinson and co-workers reported MEG induced 2-fold photocurrent enhancement in solar cells based on PbS QD-sensitized $TiO_2$ single crystals.[1] Zhu and co-workers reported hot electron injection from PbSe QDs to $TiO_2$ single crystals.[13] These reports imply ultrafast interfacial electron-transfer rates from PbSe and PbS QDs to $TiO_2$ that are competitive with the fast exciton−exciton annihilation (10−100 ps[15,16]) and the even faster hot electron relaxation (∼0.2−6 ps[17,18]) processes. However, recent time-resolved spectroscopy studies have reported interfacial electron-transfer rates on a much slower time scale (∼100 ns) in PbS-$TiO_2$ complexes[7] and a lack of hot electron transfer from PbSe to $TiO_2$ nanoparticles.[19] These discrepancies may be caused in part by different QDs and QD−$TiO_2$ linkages used in these studies. Systematic studies of the factors that control the rate of charge transfer from lead salt QDs are needed.

In this paper, we report a transient absorption (TA) study of the charge carrier separation and recombination dynamics between PbS QDs and an adsorbed electron acceptor, methylene blue ($MB^+$). TA spectroscopy in the visible region has been shown to be a powerful tool for studying charge separation dynamics from CdX (X = S, Se, Te) QDs to various acceptors (including $MB^+$), because the 1S exciton bleach in excited CdX QDs is dominated by the state filling of the 1S electron level and provides a convenient probe of the dynamics of the 1S electron.[20−25] In excited PbS QDs, both 1S electrons and holes contribute to overlapping TA features (1S exciton bleach and induced absorption) in the visible and near-IR regions that cannot be easily separated. However, we observed that the 1S electrons and holes have distinct intraband absorption features in the mid-IR, which can be used to directly follow their interfacial charge-transfer dynamics. We show that the charge separation (electron-transfer) and recombination (hole-transfer) rates are $(2.7 \pm 0.2) \times 10^{12}$ and $(1.1 \pm 0.2) \times 10^{11}$ $s^{-1}$, respectively.

The sample preparation procedures and the TA measurement setup are described in the Supporting Information (SI). The steady-state absorption spectra of PbS QDs and PbS-$MB^+$ complexes in heptane solutions are shown in Figure 1a. The PbS QDs used in this study show a first ($1S_h \rightarrow 1S_e$) exciton absorption band at 930 nm, corresponding to an estimated diameter of 3.6 nm.[26] Compared to free QDs, the QD-$MB^+$ complexes show the same QD first exciton band at 930 nm and an additional absorption feature centered at 660 nm that corresponds to the ground-state absorption of $MB^+$ molecules. The average number of $MB^+$ per QD was estimated to be ∼9, as described in the SI. Following the recent reports of Wise and co-workers,[7,26] the $1S_e$ and $1S_h$ energy levels were estimated to be −3.7 and −5.0 eV (vs vacuum), respectively, as shown in Figure 1b. Compared with the reduction potential of $MB^+$ (−4.5 eV vs vacuum),[27] the estimated Gibbs free energy changes (or driving forces) for electron transfer from the excited PbS to $MB^+$ and the subsequent charge recombination processes are −0.8 and −0.5 eV, respectively.[28,29]

To determine the charge separation and recombination rates, we measured the TA spectra of the PbS and PbS-$MB^+$

**Received:** April 11, 2011
**Published:** May 26, 2011

ACS Publications © 2011 American Chemical Society



dx.doi.org/10.1021/ja2033348 | J. Am. Chem. Soc. 2011, 133, 9246–9249

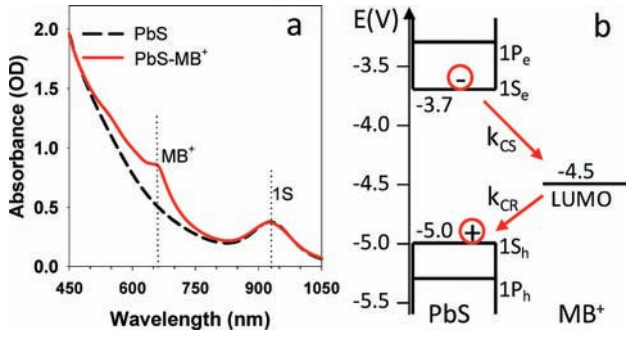


**Figure 1.** (a) UV−vis absorption spectra of free PbS QDs (black dashed line) and PbS-MB$^+$ complexes (red solid line). (b) Schematic diagram of relevant energy levels (relative to vacuum) involved in the interfacial charge separation ($k_{CS}$) and recombination ($k_{CR}$) processes in PbS-MB$^+$ complexes.

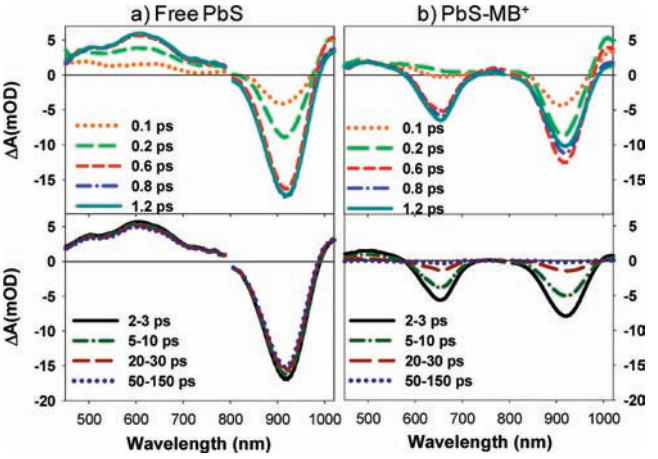


**Figure 2.** Visible and near-IR transient absorption spectra of (a) PbS QDs and (b) PbS-MB$^+$ complexes in heptane at indicated delay time windows after 800 nm excitation. Upper panels, 0.1−1.2 ps; lower panels, 2−150 ps.

complexes in the visible, near-IR, and mid-IR after 800 nm excitation. The expected processes in this system are summarized in eq 1,

$$\text{PbS}^{**}\text{-MB}^+ \xrightarrow{k_R} \text{PbS}^*(1S_e, 1S_h)\text{-MB}^+ \xrightarrow{k_{CS}} \text{PbS}^+(1S_h)\text{-MB}^\bullet \xrightarrow{k_{CR}} \text{PbS-MB}^+ \quad (1)$$

where PbS$^{**}$-MB$^+$ represents an excited complex with the QD in the initial excited state generated by the excitation pulse. It relaxes with a rate constant $k_R$ to form PbS$^*$-MB$^+$, in which the QD is in the 1S exciton state. Charge separation in the excited complex (with a rate constant $k_{CS}$) generates the charge-separated state (PbS$^+$-MB$^\bullet$), which recombines (with a rate constant $k_{CR}$) to regenerate the complex in the ground state (PbS-MB$^+$).

The visible and near-IR TA spectra of PbS and PbS-MB$^+$ measured under the same conditions are compared in Figure 2. The TA spectra of free QDs show a bleach of the 1S exciton band (~930 nm) and a broad positive band from 450 to 800 nm. The 1S exciton bleach is caused by the state-filling of the 1S electron and hole levels.[30] The broad positive absorption has been attributed to

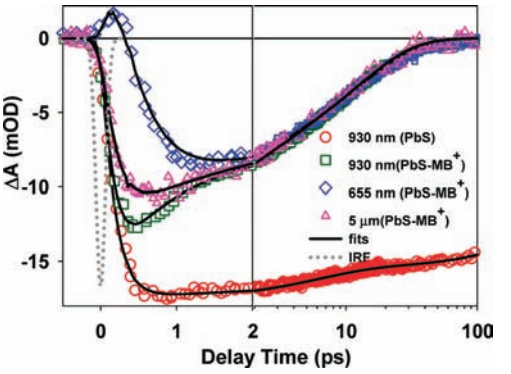


**Figure 3.** Comparison of 1S exciton bleach recovery kinetics (at 930 nm) of free PbS QDs (red circles) and PbS-MB$^+$ complexes (green squares). Also shown are the normalized kinetics of the MB$^+$ ground-state bleach (GSB at 655 nm, blue diamonds) and the $1S_h-1P_h$ intraband transition (at 5 $\mu$m, purple triangles) in PbS-MB$^+$ complexes. These kinetics were normalized to match those of the 1S exciton bleach at the later delay times. Solid lines are fits to a kinetics model described in the Supporting Information. The dotted curve is the instrument response function. The $x$ axis is in linear scale in the left panel (−0.5 to 2 ps) and in logarithmic scale in the right panel (2 to 100 ps).

the Stark effect-induced red-shift of the higher energy bands in the presence of the 1S exciton.[31−33] These exciton-induced absorption and bleach features show only a small decay (<15%) within 150 ps. It indicates that most excited QDs are in long-lived (>1 ns) single exciton states under these experimental conditions, which is in agreement with the estimated average number of excitons per QD of 0.4−0.8 (see SI).

The TA spectra of the PbS-MB$^+$ complexes (Figure 2b) show an ultrafast (<0.6 ps) formation of the MB$^+$ ground-state bleach (GSB) at 660 nm in addition to the PbS 1S exciton-induced TA features. The amplitude of the 1S exciton bleach at 0.6 ps is considerably (~30%) smaller than that in free PbS QDs under the same conditions. This can be more readily seen in Figure 3, in which the kinetic traces of the 1S exciton bleach (at 930 nm) in PbS-MB$^+$ complexes and free PbS QDs are compared. The observed ultrafast exciton bleach recovery and MB$^+$ bleach formation indicate ultrafast quenching of the PbS excitons by MB$^+$. From the energetics shown in Figure 1b, exciton quenching by hole transfer and energy transfer is not possible in this system. Therefore, it can be attributed to ultrafast electron transfer from the PbS to MB$^+$. The ET process should generate reduced MB$^+$ molecules (MB radicals) with an absorption band at around 420 nm,[25] a spectral region that is unfortunately not accessible in this study due to the strong (OD > 2) QD absorption (see Figure 1a). Further support for this assignment will be provided below by directly probing the electron and hole intraband transitions.

The TA spectra after 2 ps show the simultaneous recovery of the MB$^+$ GSB and the decay of the QD TA features (1S exciton bleach and induced absorption). As shown in Figure 3, the recovery of the MB$^+$ GSB and 1S exciton bleach follow the same kinetics, suggesting that the spectral evolution after 2 ps can be attributed to recombination of the electron in the MB radical with the 1S hole in the PbS QD (to regenerate both MB$^+$ and QD ground state). These kinetics differ at $t$ < 2 ps due to the overlapping contributions of the 1S electron-induced TA features (bleach at 930 nm and induced absorption at 655 nm) and MB$^+$ GSB. The electron-transfer process leads to the initial


dx.doi.org/10.1021/ja2033348 |J. Am. Chem. Soc. 2011, 133, 9246–9249

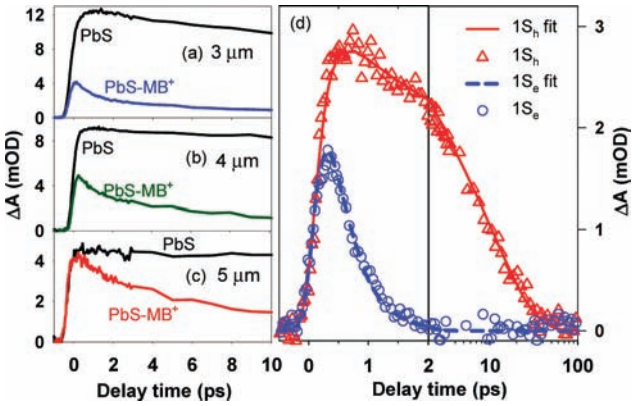


**Figure 4.** Comparison of mid-IR kinetics of free PbS QDs (black line) and PbS-$MB^+$ complexes at (a) 3.0 (blue line), (b) 4.0 (green line), and (c) 5.0 $\mu$m (red line). (d) Kinetics of 1S electrons (blue circles) and 1S holes (red triangles) in PbS-$MB^+$ complexes. The 1S hole kinetics is monitored at 5.0 $\mu$m, where the IR absorption is dominated by the $1S_h-1P_h$ transition. The 1S electron kinetics is obtained by subtracting the hole contribution to the total signal at 3.0 $\mu$m. Solid and dashed lines are fits according to eqs S4 and S5, respectively, in the Supporting Information. The $x$ axis is in linear scale in the left panel (−0.5 to 2 ps) and in logarithmic scale in the right panel (2 to 100 ps).

ultrafast recovery of the 1S electron-induced bleach at 930 nm and the formation of the $MB^+$ GSB at 655 nm. As will be discussed later, the 1S electron dynamics can be extracted by global fitting of these kinetic traces.

Clearly, the 1S exciton-induced bleach and absorption in the visible and near-IR contain contributions from both 1S electrons and holes, consistent with a previous electrochemical study of charged PbS QDs.[30] This previous study also showed that the electron ($1S_e \rightarrow 1P_e$) intraband transition in the mid-IR has a slightly higher energy than the hole ($1S_h \rightarrow 1P_h$) transitions. In this work, we utilize this energy separation to independently probe the electron and hole dynamics in the PbS-$MB^+$ complexes, enabling us to follow directly the charge separation and recombination processes, respectively. The kinetics of mid-IR absorption of free PbS QDs and PbS-$MB^+$ complexes are compared in Figure 4a−c. The free QD mid-IR absorptions are long-lived (only the first 10 ps are shown), consistent with the presence of long-lived single excitons. Similar absorptions were previously observed in PbSe QDs.[34,35] The kinetics of PbS-$MB^+$ complexes show much faster decays. The initial mid-IR absorptions in PbS-$MB^+$ are about 30% and 50% of those in free PbS QDs at 3.0 and 4.0 $\mu$m, respectively, suggesting an ultrafast decay (<0.5 ps) due to the ultrafast electron-transfer process. This ultrafast decay component is absent at 5.0 $\mu$m, where the initial signal amplitude is the same as that in free PbS QDs. Therefore, the absorption at 5.0 $\mu$m can be attributed to the hole $1S_h \rightarrow 1P_h$ intraband transition and is a direct probe of the 1S hole dynamics. This assignment is supported by the comparison in Figure 3, which shows that the kinetics at this wavelength are identical to those of the 1S exciton bleach and $MB^+$ bleach recovery after 2 ps.

As shown in Figure S1 (SI), a normalized comparison of the mid-IR absorptions at 3.0, 4.0, and 5.0 $\mu$m in PbS-$MB^+$ complexes indicates that after 2 ps these kinetics are identical and probe the population of the 1S hole (i.e., the charge recombination process). They differ in the amplitudes of the ultrafast decay component, which increases at higher energy due to an increased contribution from the electron $1S_e \rightarrow 1P_e$ transition. The electron kinetics can be obtained by subtracting the hole contribution (represented by the normalized kinetics at 5 $\mu$m) from the total signal at 3.0 $\mu$m, as shown in Figure 4d. The electron kinetics show an ultrafast decay within 2 ps, consistent with the observed ultrafast 1S exciton recovery and $MB^+$ bleach formation shown in Figures 2 and 3. Our data also suggest that it should be possible to identify a spectral window (<3 $\mu$m) that monitors only the 1S electron dynamics.

To quantify the charge separation and recombination rates in the PbS-$MB^+$ complexes, we fit the kinetics shown in Figures 3 and 4 according to eq 1. A detailed kinetics model that describes the time-dependent concentration of various species and the fitting procedure is given in the SI. The kinetics of free QDs at 930 nm were first fit to obtain the hot excited-state relaxation rate $k_R$ ($5.9 \times 10^{12}$ $s^{-1}$), which is assumed to be the same for the PbS-$MB^+$ complexes. The normalized kinetics at 5.0 $\mu$m were then fit to obtain the charge recombination rate ($k_{CR}$). Finally, the kinetics at 930 nm (1S exciton bleach), 655 nm ($MB^+$ ground state), and 3.0 $\mu$m (1S electron and hole) were fit simultaneously, with the charge separation rate ($k_{CS}$) as the only fitting parameter. As shown in Figures 3 and 4, these kinetics are well fit by this model. Biexponential functions were needed to satisfactorily describe both the charge separation and recombination kinetics, reflecting the heterogeneities of these interfacial processes. From the biexponential fits, amplitude-weighted average time constants were calculated, yielding average charge separation and recombination rates of $(2.7 \pm 0.2) \times 10^{12}$ and $(1.1 \pm 0.2) \times 10^{11}$ $s^{-1}$, respectively, in the PbS-$MB^+$ complexes. The error bars reflect standard deviations of rates determined from three sets of data.

In this fitting model, we have assumed that electron transfer occurs from the 1S electron level in PbS-$MB^+$ complexes, and compared to free PbS QDs, the ultrafast electron-transfer rate in the complexes gives rises to the reduced electron intraband absorption (Figure 4) and interband features (bleach at 930 nm and broad absorption from 450 to 800 nm, Figures 2 and 3) at early delay times. The average charge separation rate is approximately a factor of 2 slower than the electron relaxation rate, suggesting that in some of the complexes charge separation may have occurred prior to electron relaxation to the 1S level, which can also lead to the reduced 1S electron features shown in Figures 2−4. Ultrafast electron transfer and possible hot electron extraction are consistent with a recent study of PbSe QDs on $TiO_2$ single crystals, in which hot electron transfer from PbSe to $TiO_2$ and ultrafast (~10 ps) charge recombination were observed.[13] The observed ultrafast charge separation rate also suggests the possibility of dissociating multiple excitons prior to the exciton−exciton annihilation process.[9−12] Our results are also consistent with the efficient multiexciton collection reported for solar cells based on PbS QD-sensitized $TiO_2$ single crystals, assuming the charge recombination process can be suppressed under device operation conditions.[1] A recent report of the formation of a depleted heterojunction between PbS and $TiO_2$ offers a possible mechanism for preventing the charge recombination process in these devices.[3] It should be pointed out that the driving force for electron transfer from PbS to $MB^+$ is considerably larger than that to $TiO_2$. Direct TA measurement of charge separation rates at the PbS and PbSe/$TiO_2$ interfaces, which is ongoing, should offer a better comparison with the reported hot electron injection and multiexciton collection in these materials.[1,13] Our study demonstrated that charge separation and recombination processes can be directly measured by monitoring the electron

and hole intraband transitions. This approach should be generally applicable to lead salt and other QDs.[36]

In summary, charge separation and recombination in PbS-$MB^+$ complexes have been studied by transient absorption spectroscopy. While the 1S electron and hole contribute to overlapping TA features in the visible and near-IR regions, they have distinct intraband transitions in the mid-IR that can be used to follow their dynamics independently. We show that the charge separation and recombination rates are $(2.7 \pm 0.2) \times 10^{12}$ and $(1.1 \pm 0.2) \times 10^{11}$ $s^{-1}$, respectively. The ultrafast charge separation rate suggests the possibility of hot electron injection and multiexciton dissociation from these strongly quantum confined QDs, consistent with recent reports of these phenomena.[1,13]

## ■ ASSOCIATED CONTENT

**Supporting Information.** Experimental methods and data fitting procedures. This material is available free of charge via the Internet at http://pubs.acs.org.

## ■ AUTHOR INFORMATION

**Corresponding Author**
tlian@emory.edu

## ■ ACKNOWLEDGMENT

This work was supported by the National Science Foundation (CHE-0848556) and Petroleum Research Fund (PRF no. 49286-ND6).

## ■ REFERENCES

(1) Sambur, J. B.; Novet, T.; Parkinson, B. A. *Science* **2010**, *330*, 63.
(2) Sargent, E. H. *Nat. Photon.* **2009**, *3*, 325.
(3) Pattantyus-Abraham, A. G.; Kramer, I. J.; Barkhouse, A. R.; Wang, X.; Konstantatos, G.; Debnath, R.; Levina, L.; Raabe, I.; Nazeeruddin, M. K.; Gratzel, M.; Sargent, E. H. *ACS Nano* **2010**, *4*, 3374.
(4) Luther, J. M.; Law, M.; Beard, M. C.; Song, Q.; Reese, M. O.; Ellingson, R. J.; Nozik, A. J. *Nano Lett.* **2008**, *8*, 3488.
(5) Hines, M. A.; Scholes, G. D. *Adv. Mater.* **2003**, *15*, 1844.
(6) Murray, C. B.; Sun, S.; Gaschler, W.; Doyle, H.; Betley, T. A.; Kagan, C. R. *IBM J. Res. Dev.* **2001**, *45*, 47.
(7) Hyun, B.-R.; Zhong, Y.-W.; Bartnik, A. C.; Sun, L.; Abruña, H. D.; Wise, F. W.; Goodreau, J. D.; Matthews, J. R.; Leslie, T. M.; Borrelli, N. F. *ACS Nano* **2008**, *2*, 2206.
(8) Leventis, H. C.; O'Mahony, F.; Akhtar, J.; Afzaal, M.; O'Brien, P.; Haque, S. A. *J. Am. Chem. Soc.* **2010**, *132*, 2743.
(9) Pijpers, J. J. H.; Ulbricht, R.; Tielrooij, K. J.; Osherov, A.; Golan, Y.; Delerue, C.; Allan, G.; Bonn, M. *Nat. Phys.* **2009**, *5*, 811.
(10) McGuire, J. A.; Sykora, M.; Joo, J.; Pietryga, J. M.; Klimov, V. I. *Nano Lett.* **2010**, *10*, 2049.
(11) Beard, M. C.; Midgett, A. G.; Hanna, M. C.; Luther, J. M.; Hughes, B. K.; Nozik, A. J. *Nano Lett.* **2010**, *10*, 3019.
(12) Nair, G.; Geyer, S. M.; Chang, L.-Y.; Bawendi, M. G. *Phys. Rev. B* **2008**, *78*, No. 125325.
(13) Tisdale, W. A.; Williams, K. J.; Timp, B. A.; Norris, D. J.; Aydil, E. S.; Zhu, X.-Y. *Science* **2010**, *328*, 1543.
(14) Nozik, A. J. *Physica E: Low-Dimens. Syst. Nanostruct.* **2002**, *14*, 115.
(15) Schaller, R. D.; Sykora, M.; Pietryga, J. M.; Klimov, V. I. *Nano Lett.* **2006**, *6*, 424.
(16) Klimov, V. I.; McGuire, J. A.; Schaller, R. D.; Rupasov, V. I. *Phys. Rev. B* **2008**, *77*, No. 195324.
(17) Schaller, R. D.; Pietryga, J. M.; Goupalov, S. V.; Petruska, M. A.; Ivanov, S. A.; Klimov, V. I. *Phys. Rev. Lett.* **2005**, *95*, 196401/1.
(18) Harbold, J. M.; Du, H.; Krauss, T. D.; Cho, K. S.; Murray, C. B.; Wise, F. W. *Phys. Rev. B* 2005, *72*, No. 195312.
(19) Pijpers, J. J. H.; Koole, R.; Evers, W. H.; Houtepen, A. J.; Boehme, S.; Donega, C. D.; Vanmaekelbergh, D.; Bonn, M. *J. Phys. Chem. C* **2010**, *114*, 18866.
(20) Burda, C.; Link, S.; Mohamed, M.; El-Sayed, M. *J. Phys. Chem. B* **2001**, *105*, 12286.
(21) Klimov, V. I. *Annu. Rev. Phys. Chem.* **2007**, *58*, 635.
(22) Robel, I.; Kuno, M.; Kamat, P. V. *J. Am. Chem. Soc.* **2007**, *129*, 4136.
(23) Zhu, H.; Song, N.; Lian, T. *J. Am. Chem. Soc.* **2010**, *132*, 15038.
(24) Huang, J.; Stockwell, D.; Huang, Z.; Mohler, D. L.; Lian, T. *J. Am. Chem. Soc.* **2008**, *130*, 5632.
(25) Huang, J.; Huang, Z. Q.; Yang, Y.; Zhu, H. M.; Lian, T. Q. *J. Am. Chem. Soc.* **2010**, *132*, 4858.
(26) Kang, I.; Wise, F. W. *J. Opt. Soc. Am. B* **1997**, *14*, 1632.
(27) Kamat, P. V.; Dimitrijevic, N. M.; Fessenden, R. W. *J. Phys. Chem.* **1987**, *91*, 396.
(28) Brus, L. *J. Chem. Phys.* **1983**, *79*, 5566.
(29) Brus, L. E. *J. Chem. Phys.* **1984**, *80*, 4403.
(30) Wehrenberg, B. L.; Guyot-Sionnest, P. *J. Am. Chem. Soc.* **2003**, *125*, 7806.
(31) Kohn, S. E.; Yu, P. Y.; Petroff, Y.; Shen, Y. R.; Tsang, Y.; Cohen, M. L. *Phys. Rev. B* **1973**, *8*, 1477.
(32) Kanazawa, H.; Adachi, S. *J. Appl. Phys.* **1998**, *83*, 5997.
(33) Cho, B.; Peters, W. K.; Hill, R. J.; Courtney, T. L.; Jonas, D. M. *Nano Lett.* **2010**, *10*, 2498.
(34) Ji, M.; Park, S.; Connor, S. T.; Mokari, T.; Cui, Y.; Gaffney, K. J. *Nano Lett.* **2009**, *9*, 1217.
(35) Ellingson, R. J.; Beard, M. C.; Johnson, J. C.; Yu, P.; Micic, O. I.; Nozik, A. J.; Shabaev, A.; Efros, A. L. *Nano Lett.* **2005**, *5*, 865.
(36) Guyot-Sionnest, P. *Struct. Bonding* **2005**, *118*, 59.